Journal of Cleaner Production 316 (2021) 128340

Contents lists available at ScienceDirect

Journal of Cleaner Production

journal homepage: www.elsevier.com/locate/jclepro

Valorization of olive mill solid residue through ultrasound-assisted extraction and phenolics recovery by adsorption process

S. Mehdi Niknam, Mansoore Kashaninejad, Isabel Escudero, M. Teresa Sanz, Sagrario Beltrán, José M. Benito *

Department of Biotechnology and Food Science, University of Burgos, Plaza Misael Bañuelos s/n, 09001, Burgos, Spain

ARTICLE INFO

Handling editor: Zhen Leng

Keywords:
Olive pomace
Ultrasound-assisted extraction
Response surface methodology
Phenolics adsorption-desorption

ABSTRACT

Olive pomace, a solid residue generated during olive oil production process and a rich source of phenolic compounds, was dried and defatted to obtain a pomace oil rich in monounsaturated fatty acids with 64% oleic acid. The defatted pomace was further treated by ultrasound-assisted extraction (UAE). The optimal phenol extraction conditions of 10 min, 40% amplitude and 4% (w/v) solid:solvent ratio, yielded to 14.70 mg/g total phenols, 2.48 mg/g total flavonoids and 0.924 mmol Trolox/g antioxidant activity. In order to purify valuable biophenols, two polymeric resins (XAD4 and XAD16) and two activated charcoals (NPAC and GAC) were tested as adsorbents using a magnetic stirrer and an incubator shaker. XAD16 (100 g/L) in magnetic stirrer showed the optimal adsorption ratios with 74.36%, 39.25%, 68.79% and 100% for total phenols, hydroxytyrosol, tyrosol and oleuropein, respectively. Desorption using acidified 50% (v/v) ethanol-water at pH = 2.3 proved 57.65% recovery of total phenols, 19.27% of hydroxytyrosol and 45.73% of tyrosol. These results indicate that extraction and selective purification of biophenols from olive pomace can be achieved by the proposed UAE using 50% v/v ethanol-water as solvent, followed by adsorption-desorption stages with the XAD16 polymeric resin.

1. Introduction

Olive mill wastes are very well known for their significant negative impact on the environment. They are generated during the extraction of olive oil by means of a press, a two-phase centrifuge or a three-phase centrifuge system. The three-phase system, used in most of the olive oil producing countries including Iran, generates a solid husk, oil, and a huge volume of foul smelling acidic dark liquid called olive mill wastewater (OMWW), while the two-phase system releases a wet olive husk and oil (Gebreyohannes et al., 2016). This last system is the one used mainly in Spain, the leader in olive tree cultivation (Manzanares et al., 2017) where, according to the estimations from FAOSTAT (2021), 2.6 Mha of olive crop were cultivated in 2019, representing 24.5% of total worldwide production. The treatment and disposal of such a huge volume of solid and liquid wastes is a very critical problem, due to their high content of organic matter and phenolics (Khoufi et al., 2011; Tsagaraki and Lazarides, 2012).

Although being lignocellulosic material (mainly olive peel, pulp and pits), the solid waste is of heterogeneous nature. It contains 4–15% of olive pomace oil (depending on the olive cultivation region and the employed extraction method) and can be found along with many chemical compounds, such as alkaline (potassium) and alkaline-earth (calcium and magnesium) metals, sugars and polyphenols, which come from the vegetation water (Sánchez Moral and Ruiz Méndez, 2006). The conversion of olive mill solid wastes can be directed to heat and power production by thermochemical processes (Parascanu et al., 2018), or be upgraded into added-value products by biochemical/chemical treatments.

The antioxidant activity of OMWW and olive pomace has been widely studied and demonstrated (Alu'datt et al., 2010; Lafka et al., 2011). Since only 2% of the phenolic compounds in the olives are transferred to the oil and up to 98% are retained in the wastes, olive pomace has been considered to be an affordable and abundant source of biologically active phenolic compounds that have promising potential as antioxidant, anti-inflammatory and antimicrobial agents (Suárez et al., 2009). However, the qualitative and quantitative heterogeneity of phenolic compounds in these by-products is often a difficulty in finding viable applications in this area.

The main component of the phenolic fraction found in olive mill

* Corresponding author.
E-mail addresses: snx1002@alu.ubu.es (S.M. Niknam), mkx1002@alu.ubu.es (M. Kashaninejad), iescuder@ubu.es (I. Escudero), tersanz@ubu.es (M.T. Sanz), beltran@ubu.es (S. Beltrán), jmbmoreno@ubu.es (J.M. Benito).

https://doi.org/10.1016/j.jclepro.2021.128340
Received 23 March 2021; Received in revised form 18 June 2021; Accepted 14 July 2021
Available online 15 July 2021

Nomenclature

A	adsorption ratio
C	constant in the particle diffusion kinetic model
C_0	initial phenol concentration (after ethanol evaporation)
C_D	concentration of phenolic compounds in the filtrate after desorption
C_e	equilibrium concentration of phenolic compounds
D	desorption ratio
E	energy input
k_1	rate constant for the pseudo-first order kinetic model
k_2	rate constant for the pseudo-second order kinetic model
k_d	rate constant for the particle diffusion kinetic model
m	mass
PD	ultrasonic power density
Q_e	adsorption content
q_e	amount of phenolic compounds adsorbed at equilibrium
q_t	amount of phenolic compounds adsorbed at time t
R	total recovery
R^2	coefficient of determination
t	time
V_0	volume of the initial sample
V_D	volume of the filtrate after desorption
W	weight of adsorbent
X	input variable factor (independent variable)
Y	response variable

Abbreviation

AA	antioxidant activity
AC	activated charcoal
ANOVA	analysis of variance
CCD	central composite design
EOP	extracted olive pomace
FAMEs	fatty acid methyl esters
GAC	granulated activated charcoal
GAE	gallic acid equivalents
HT	hydroxytyrosol
LCA	life cycle assessment
LSD	least significant difference test
MLR	multiple linear regressions
MUFA	monounsaturated fatty acid
NPAC	Norit powdered activated charcoal
OLE	oleuropein
OMWW	olive mill wastewater
PUFA	polyunsaturated fatty acid
QE	quercetin equivalents
RSM	response surface methodology
S:S	solid:solvent ratio
SFA	saturated fatty acid
TFC	total flavonoid content
TPC	total phenolic content
TY	tyrosol
UAE	ultrasound-assisted extraction
USM	unsaponifiable matter

wastes is hydroxytyrosol, part of which comes from oleuropein, the most abundant phenol present in olive trees, through an esterase-mediated cleavage during oil extraction. Hydroxytyrosol is a potent antioxidant, with proven abilities to scavenge oxygen and nitrogen free radicals, to inhibit low-density lipoprotein oxidation, platelet aggregation, endothelial cell activation, and to protect against DNA damage (Hu et al., 2014; Zhang et al., 2009). Despite these important properties, hydroxytyrosol is not commercially available in large amounts since all the synthetic or extractive developed routes have resulted to be cumbersome, expensive, or not eco-sustainable (Espín et al., 2001; Fava et al., 2017). Polyphenols recovery is a key point for the valorization of these solid residues and would support a more sustainable bioeconomy, reducing environmental problems caused by these wastes and making them suitable for commercialization.

Ultrasound-assisted extraction (UAE) technology is recommended for the recovery of valuable organic compounds. The high shear forces generated by sonic waves promote extraction by enhancing mass transfer (Chemat et al., 2017b; Misra et al., 2018) due to cavitation and streaming (Leighton, 2007), with an internal convection motion of solute within the solvent inside holes of porous material (Allaf et al., 2013). UAE is one of the best non-thermal technologies from an environmental point of view (Chemat et al., 2017a) with several advantages, including reduced extraction time, energy, and solvent usage. The solid/liquid ratio can significantly affect the extraction yield and UAE parameters as amplitude and pressure can be easily tuned as a function of the target specific objectives (Chemat et al., 2020). Ultrasound irradiation (20–100 kHz) offers high reproducibility in shorter time (Ma et al., 2008, 2009; Sun et al., 2011), reduced solvent consumption and less energy input (Chemat et al., 2008). Moreover, the ultrasound energy in extraction also provides more effective mixing, faster energy transfer, reduced thermal gradients, and lower extraction temperature requirement (Azmir et al., 2013).

Adsorption is an efficient technology for the selective removal, recovery and separation of some compounds that requires a relatively low economic investment (Kammerer et al., 2010). It is one of the most commonly applied processes for the recovery of polyphenols from plant extracts that is gaining increasing importance in food industry. Adsorption is attractive for its relative simplicity of design, operation and scale-up, but its major drawbacks include limited selectivity, the need to regenerate the adsorbent for reuse, and loss of capacity after several cycles (Kaleh and Geiβen, 2016). In recent years, several studies dealt with the uptake of polyphenols and other bioactive compounds from olive mill wastes on different adsorbents (Yangui et al., 2017a, 2017b; Zagklis et al., 2015).

The current study was carried out in two parts. First, olive mill solid residue (olive pomace) was dried and defatted, and subsequently processed with UAE under optimal conditions, which were estimated by using response surface methodology. Thence, multiple adsorption-desorption processes were performed on the olive pomace extracts obtained. For this study, XAD4 and XAD16 polymeric resins and two different types of activated charcoals were tested as adsorbents. Furthermore, several desorption solvents were also tested and evaluated in terms of total phenols recovery and also selective isolation of hydroxytyrosol, tyrosol and oleuropein, which are the main components of the phenolic fraction present in olive mill wastes.

2. Materials and methods

2.1. Samples and chemicals

Olive mill solid residues, obtained by means of a three-phase centrifugal extraction process, were kindly provided by the Mamalan Agro Industrial Company (Tarom county, Zanjan, Iran). Folin-Ciocalteu reagent, acetic acid, isooctane, n-hexane and acetonitrile were purchased from VWR International Eurolab (Barcelona, Spain). Sodium carbonate, gallic acid, 1,1-diphenyl-2-picrylhydrazyl (DPPH), 6-hydroxy-2,5,7,8-tetramethylchroman-2-carboxylic acid (Trolox), quercetin, aluminum chloride, methanol, ethanol, potassium acetate, hydrochloric acid (HCl, 37%), ammonium acetate, hydroxytyrosol, tyrosol, oleuropein, methyltricosanoate and other standards of fatty acid methyl esters were

Table 1
Characteristics of the adsorbents used in this work.

Adsorbent	Dry density (g/mL)	Mesh	Mean pore size (Å)	Particle diameter (mm)	Specific surface (m^2/g)
XAD4 polymeric resin	1.02	20–60	40	0.25–0.84	725
XAD16 polymeric resin	1.02	20–60	200	0.25–0.84	900
Norit powdered activated charcoal (NPAC)	0.25–0.60			0.15–0.25	1000
Granulated activated charcoal (GAC)	2–2.1			1–3	900–1200

purchased from Sigma-Aldrich (Darmstadt, Germany). Amberlite® XAD4 and XAD16 polymeric resins were provided from Fluka (Germany), which have been reported to yield satisfactory adsorption results for phenolic compounds in previous works (Frascari et al., 2019; Pinelli et al., 2016; Zagklis and Paraskeva, 2018). Powdered activated charcoal (NPAC, Norit-97876, Sigma-Aldrich, Darmstadt, Germany) and granulated activated charcoal (GAC, CA03461000, Scharlau, Barcelona, Spain) were also tested as adsorbents as they have been also used in previous works (Fava et al., 2017; Richard et al., 2009; Ziati et al., 2017). Characteristics of all adsorbents are shown in Table 1.

2.2. Olive pomace pretreatment

Olive pomace was dried at 60 °C for 24 h in an oven (model 2600210, JP Selecta, Barcelona, Spain) to remove most of their moisture (about 55–60% w/w). This temperature was selected to avoid the degradation of phenolic compounds. In the study performed by Santos et al. (2014) phenolic content and antioxidant activity of pears of Rocha variety from five different locations were evaluated and dried at different temperatures (40 and 60 °C). Although the amounts of phenolic compounds were not very much affected, the antioxidant activity suffered a decrease with drying at both temperatures when compared to that of the fresh pears. In addition, the effect of drying temperature on antioxidant activity, total phenolic content, fatty acid composition and tocopherol content of citrus seeds and seed oils were studied by Al Juhaimi et al. (2018), concluding that all of them suffered a severe decrease for drying temperatures above 60 °C.

Dried olive pomace was then ground by using a coffee grinder to obtain an average particle diameter of about 1 mm. For applying defatting process, Soxhlet method was performed using a B-811 extraction system (BÜCHI Labortechnik AG, Flawil, Switzerland). The ground olive cake (about 20 g, 5 g in each of the 4 extraction chambers) was placed in the Soxhlet apparatus and continuously refluxed with 400 mL (100 mL for each chamber) of n-hexane for 25 cycles (at 70 °C for 3 h). After oil extraction, n-hexane was distilled and recovered using the same system. The obtained oil was weighed resulting into an average recovery yield of 12.98%. Then the pretreated olive pomace samples were kept in darkness at −20 °C for further use.

2.3. Analysis of fatty acid profile

The fatty acid content of the extracted oil was analyzed by gas chromatography (GC) using the AOAC 991.39 (1995) official method, which is based on the breakdown of all glycerides and subsequent derivatization to fatty acid methyl esters (FAMEs). These FAMEs were analyzed by using an Agilent 6890N Network GC system equipped with a flame ionization detector (FID) and a fused silica capillary column (Omegawax™ 320, 30 m × 0.32 mm i.d.). The separation was performed with helium as carrier gas (1.8 mL/min). The chromatographic conditions were as follows: initial column temperature of 180 °C for 15 min, heated to 200 °C at 1 °C/min, held at 200 °C for 1 min, heated again to 220 °C at 5 °C/min, and finally held at 220 °C for 15 min. A split injector (50:1) at 250 °C was used and the FID was also heated to 250 °C. The injection volume was 1 μL.

FAMEs where identified by comparison of their retention times with those of chromatographic standards and their quantification was made by using methyl tricosanoate (C23:0; 1 mg/mL dissolved in isooctane) as internal standard. Two replicates were prepared for each sample.

2.4. Ultrasound-assisted extraction of phenolic compounds

Extraction of phenolic compounds was carried out by placing the pretreated olive pomace samples (1.6–1.8 g) in Falcon centrifuge tubes and mixing with 40 mL of 50% v/v ethanol-water solvent for each experiment. Then, these tubes containing samples were entered to a high intensity ultrasonic homogenizer (Sonics VCX500, 500 W, 20 kHz, Newtown, CT, USA) equipped with a titanium alloy microtip probe of 3 mm diameter, where UAE was performed at 30 °C with ultrasound pulses every 5 s (5 s on and 5 s off). Different experimental conditions of sonication time, amplitude (maximum 40%, as indicated by the manufacturer for the selected probe), and solid:solvent (S:S) ratio were applied based on the design of experiments described below.

The ultrasonic power density (PD) was evaluated as:

$$PD = \frac{E}{t\ m} \quad (1)$$

where E is the energy input (J), t is the ultrasonication time (s) and m is the defatted olive pomace mass (g). In this work, the ultrasonic power density varied from 0.12 to 3.95 J/s g.

After UAE, phenolic loaded extracts were centrifuged at 12500×*g* for 10 min (Eppendorf centrifuge model 5804, Hamburg, Germany). The supernatants were filtered using 0.45 μm Millipore syringe filters and stored at −20 °C for further analysis.

2.5. Experimental design

Data were analyzed using response surface methodology (RSM) with central composite design 2^3 + star (CCD) model by the application of Statgraphics version 18 software (Statgraphics Technologies, Inc, Warrenton, VA, USA). The effects of three input variable factors: time (X_1: 2–10 min), solid:solvent (S:S) ratio (X_2: 4–20% w/v), and amplitude (X_3: 20–40%) on the phenolic extraction process was studied. Three response variables were analyzed: total phenolic content (TPC = Y_1), total flavonoid content (TFC = Y_2) and antioxidant activity (AA = Y_3). The model generated 16 experimental runs with two replicates in central point. A second-degree polynomial equation, Eq. (2), was used to express predicted responses (Y_1–Y_3) as a function of the independent variables under study (X_1-X_3).

$$Y = a_0 + a_1X_1 + a_2X_2 + a_3X_3 + a_{11}X_1^2 + a_{22}X_2^2 + a_{33}X_3^2 + a_{12}X_1X_2 + a_{13}X_1X_3 + a_{23}X_2X_3 \quad (2)$$

where Y represents the particular response variable, a_0 is a constant, and a_i, a_{ii}, a_{ij} are the linear, quadratic and interactive coefficients, respectively. The value of the factors and their effect on the responses was determined by analysis of variance (ANOVA) and LSD (least significant difference) test. The model was adjusted by means of multiple linear regressions (MLR) and its validity was determined by ANOVA. The level of significance of each coefficient was evaluated through the values of the statistical parameters F and p (probability) with a 95% confidence level (Ghorbannezhad et al., 2016).

2.6. Resin pretreatment process

The polymeric resins (XAD4 and XAD16) were pretreated using the following procedure. Resins were first washed with distilled water and after getting dried were soaked and stirred in acetone at 150 rpm for 6 h. Then, they were vacuum filtered and dried at room temperature. This step ensured the removal of organic impurities that could be trapped in them. Subsequently, resins were rinsed in ethanol with a ratio of 5 mL ethanol/g resin at 150 rpm for 2 h. After complete ethanol removal, distilled water was used to wash the resins thrice. Finally, pretreated resins were dried in an oven at 50 °C to constant weight (Kaleh and Geiβen, 2016; Zagklis and Paraskeva, 2018).

2.7. Adsorption and desorption processes

2 L of olive pomace extract were obtained under optimal operating conditions determined by experimental design. Subsequently, the ethanolic part (1 L) of the extract was evaporated by using a Heidolph Laborota 4001 rotary evaporator system (Heidolph, Schwabach, Germany) at 30 °C and 100 mmHg (0.13 bar) for 3 h. Then, the remaining dealcoholized extract was acidified to pH = 2.8 by using hydrochloric acid (HCl, 37%) and stored at 4 °C before use in adsorption tests.

In the adsorption experiments, 1.5 and 3 g of adsorbent (pretreated resin or activated charcoal) were mixed with 30 mL of dealcoholized and acidified olive pomace extract in 50 mL flasks (50 and 100 g adsorbent/L sample). All the flasks were shaken in an incubator shaker (Model G25, New Brunswick, USA) and magnetic stirrer at a shaking speed of 150 rpm for 3 h at room temperature. After adsorption runs reached equilibrium, adsorbents were separated by vacuum filtration and filtrates were analyzed.

Preliminary experiments were performed in order to select the activated charcoal (NPAC or GAC) used in this research. Therefore, adsorption experiments were performed with 50 g activated charcoal/L sample content in both magnetic stirrer and incubator shaker for 3 h. After selecting the optimal type of activated charcoal, experiments were continued to determine the optimal device and operating conditions for adsorption process. For this purpose, three adsorbents (XAD4, XAD16 and NPAC) with two input contents of 50 and 100 g adsorbent/L sample were used, resulting to six experimental runs performed with each device. The adsorption related results were quantified by using the following mass balances indicated in Eqs. (3) and (4) (Wang et al., 2017; Yang et al., 2016):

$$Q_e = \frac{(C_0 - C_e)V_0}{W} \tag{3}$$

$$A = \frac{(C_0 - C_e)}{C_0} \times 100 \tag{4}$$

where adsorption content (Q_e) is the equilibrium adsorption capacity (mg phenols/g adsorbent) and C_0 and C_e refer to the initial (in acidified optimal olive pomace extract after ethanol evaporation) and equilibrium concentrations (mg phenols/mL sample), respectively. A is the adsorption ratio (%), V_0 is the volume of the initial sample (mL) and W is the weight of the adsorbent (g).

After each run, the adsorbents used were vacuum filtered and total phenolic content (TPC) was measured in the filtrates. In addition to TPC, hydroxytyrosol, tyrosol and oleuropein contents were also measured in the filtrates obtained from adsorption process.

In desorption process, filtered adsorbents were mixed with 30 mL of ethanol and stirred in a magnetic stirrer at 150 rpm for 2 h. The volume of used solvent in desorption was the same as the initial sample volume in adsorption process. Ethanol was repeatedly used as desorption solvent in bibliography (Fava et al., 2017; Wang et al., 2017). After each run, adsorbents were vacuum filtered and phenol loaded ethanol was collected to determine the content of TPC, hydroxytyrosol, tyrosol and oleuropein. The desorption capacity was evaluated as follows (Wang et al., 2017; Yang et al., 2016):

$$D = \frac{C_D V_D}{(C_0 - C_e)V_0} \times 100 \tag{5}$$

$$R = \frac{C_D V_D}{C_0 V_0} \times 100 \tag{6}$$

where D is the desorption ratio (%), C_D is the concentration of solute in the filtrate after desorption (mg/mL) and V_D is the volume of this filtrate (mL). R is the total recovery (%), which shows the ratio of final contents of responses after desorption compared to the initial content in acidified optimal olive pomace extract after ethanol evaporation.

2.8. Adsorption kinetics

The adsorption kinetic models were studied on NPAC and two selected resins (XAD4, XAD16). The kinetic evaluation was conducted in a magnetic stirrer at 150 rpm and at room temperature. Then, aliquots (1.0 mL) of supernatant from each solution were taken at the time points of 30, 60, 90, 120, 150 and 180 min, and their total phenolic content (TPC) were measured to obtain the kinetic curves. Three models were checked to evaluate the adsorption kinetic mechanisms of phenolic compounds (Wang et al., 2017; Yang et al., 2016).

Pseudo-first-order kinetic equation:

$$\ln (q_e - q_t) = -k_1 t + \ln q_e \tag{7}$$

Pseudo-second-order kinetic equation:

$$\frac{1}{q_t} = \frac{1}{k_2 q_e^2} \times \frac{1}{t} + \frac{1}{q_e} \tag{8}$$

Particle diffusion kinetic equation:

$$q_t = k_d\, t^{1/2} + C \tag{9}$$

where q_e and q_t are the amount of phenolic compounds adsorbed at equilibrium and at time t (mg phenols/g adsorbent), respectively. k_1, k_2 and k_d are the rate constants for the pseudo-first order, pseudo-second order and particle diffusion kinetic models, respectively, and C stood for the constant in the particle diffusion kinetic model.

2.9. Analytical methods

Antioxidant activity (AA) and of total phenolic content (TPC) of the samples were measured following the DPPH method (Shen et al., 2010) and the Folin-Ciocalteu standard method (Hoff and Singleton, 1977), respectively, with some modifications, as indicated in a previous work (Niknam et al., 2020). Total flavonoid content (TFC) was measured following the procedure described by Chang et al. (2002). All tests were performed at least in duplicate and the results were averaged. Antioxidant activity was expressed as millimoles of Trolox equivalents per gram of olive pomace (mmol Trolox/g). TPC was expressed as milligrams of gallic acid equivalents per gram of olive pomace (mg GAE/g) for phenolic extraction experiments and milligrams of gallic acid equivalents per liter of olive extract (mg GAE/L) for adsorption-desorption results. TFC was expressed as milligrams of quercetin equivalents per gram of olive pomace (mg QE/g).

Phenolic compounds present in extracts were analyzed by chromatography using a HPLC-DAD Agilent 1110 (Agilent Technologies, Inc., USA) equipped with a Kinetex® 5 μm Biphenyl 100 Å column of 250 × 4.6 mm (Phenomenex Inc., CA, USA.). Separation was achieved using a linear gradient of two solvents: solvent A (5 mol/m^3 ammonium acetate with 1% (v/v) acetic acid in water) and solvent B (5 mol/m^3 ammonium acetate with 1% (v/v) acetic acid in acetonitrile). A linear increase of solvent B was used, starting with 2% of B for 7 min and then increasing from 2% to 8% B in 20 min, from 8% to 10% B in 35 min, from 10% to

Table 2
Fatty acid profile of extracted olive pomace oil.

Type of acid	Formula	Name	Fatty acid concentration Cx (mg/g)	wt. %	Acceptable ranges for olive pomace oil (Codex Alimentarius, 2013) (% of total fatty acids)
SFA	C16:0	Palmitic acid	89.1 ± 39	13.6 ± 0.01	7.5–20
MUFA	C16:1n-7	Palmitoleic acid	5.8 ± 3	0.9 ± 0.01	0.3–3.5
SFA	C18:0	Stearic acid	19.2 ± 8	2.9 ± 0.01	0.5–5
MUFA	C18:1n-9	Oleic acid	420 ± 183	64.1 ± 0.18	55–83
MUFA	C18:1n-7	Vaccenic acid	14.6 ± 6	2.2 ± 0.04	–
PUFA	C18:2n-6	Linoleic acid	89.3 ± 39	13.6 ± 0.06	3.5–21
PUFA	C18:3n-3	Alpha linolenic acid	4.6 ± 2	0.7 ± 0.01	–
SFA	C20:0	Arachidic acid	3.4 ± 1.0	0.5 ± 0.0	0.0–0.6
MUFA	C20:1n-9	Gondoic acid	1.8 ± 1.0	0.3 ± 0.0	0.0–0.4
SFA	C22:0	Behenic acid	1.4 ± 1.0	0.2 ± 0.0	0.0–0.3
SFA	C24:0	Lignoceric acid	1.4 ± 1.0	0.2 ± 0.01	0.0–0.2
MUFA	C24:1	Nervonic acid	3.7 ± 0.0	0.6 ± 0.26	–
Total fatty acids			654.5 ± 283	100 ± 0.6	

SFA: Saturated fatty acid; MUFA: Monounsaturated fatty acid; PUFA: Polyunsaturated fatty acid.

18% B in 55 min, from 18% to 38% B in 65 min, from 38% to 65% B in 75 min, and finally from 65% to 80% B in 80 min, at a flow rate of 0.8 mL/min and a column temperature of 25 °C. UV–vis detection was done at 240, 280, 330, 350, and 370 nm. Before injection, extracts were filtered through 0.45 μm pore size Millipore syringe filters. The injection volume was 40–80 μL. All tests were performed in duplicate and the results were averaged. The evaluation of the phenolic compounds was based on the comparison of the retention time of each peak and its intensity with those of the individual standards. The content of hydroxytyrosol, tyrosol and oleuropein is expressed as milligrams per liter of olive extract (mg/L).

3. Results and discussion

3.1. Characterization of extracted olive pomace oil

The commercial value of olive pomace depends on its oil content, whose composition is similar, but not identical, to that of typical olive oil (Akay et al., 2015). A mixture of saturated (SFA), monounsaturated (MUFA) and polyunsaturated fatty acids (PUFA) composes the lipid fraction of the olive pomace. As this fraction is essentially rich in MUFA, its susceptibility to oxidation is reduced. Additionally, the presence of vitamin E, a potent liposoluble antioxidant, protects long chain fatty acids against oxidative damage (Uribe et al., 2013). Important olive components that remain in olive pomace, as MUFA, pigments, vitamin E, and phenolic compounds, may act synergistically, making this oil more stable than others (Allalout et al., 2009; Antónia Nunes et al., 2018).

Table 3
Central composite design (CCD) matrix for ultrasound-assisted extraction of phenolic compounds from olive pomace.

Run	Operating conditions			Total phenolic content (mg GAE/g)	Total flavonoid content (mg QE/g)	Antioxidant activity (mmol Trolox/g)
	Time (min)	S:S ratio (%)	Amplitude (%)			
1	10	4	40	14.70	2.48	0.924
2	2	4	20	12.17	1.87	0.936
3	6	12	20	7.04	1.35	0.870
4	2	20	20	6.45	1.43	0.685
5	10	4	20	10.72	1.50	0.883
6	6	12	30	7.77	1.92	0.859
7	10	12	30	7.61	1.77	0.866
8	6	4	30	13.30	1.99	0.920
9	6	12	30	9.16	1.71	0.774
10	2	4	40	13.35	2.06	0.948
11	6	20	30	7.29	1.73	0.537
12	2	20	40	6.92	1.53	0.697
13	10	20	40	8.55	1.72	0.759
14	2	12	30	7.99	1.37	0.865
15	6	12	40	11.48	2.63	0.820
16	10	20	20	5.49	1.25	0.749

A gas chromatography analysis was performed on the oil recovered from the dry olive pomace defatting process. The fatty acid profile is reported in Table 2, which shows that the main fatty acids are oleic acid (64.10 ± 0.18%), linoleic acid (13.60 ± 0.06%) and palmitic acid (13.60 ± 0.01%). Results agree with those of the literature for olive products and by-products (Orsavova et al., 2015; Uribe et al., 2014).

Currently, the growing interest in olive pomace oil is due to its minor bioactive components that are generally included in the unsaponifiable matter (USM). USM contains significant amounts of sterols, fatty alcohols, tocopherols, triterpene alcohols and squalene. Most of these compounds possess a wide range of interesting bioactive or nutritional properties. Its functional properties are also interesting, that is, anti-inflammatory, antibacterial, antifungal, antiulcer and antitumor activity (Alu'datt et al., 2010). It must be noted that the olive pomace oil has higher content in USM than the olive oil and it is also richer in individual sterols and polyunsaturated fatty acids like linoleic acid (Rodríguez-Gutiérrez et al., 2012).

However, it should be noted that this olive pomace oil must undergo a refining process (including neutralization, winterizing, discoloration and deodorization stages) prior to use for human consumption, and many of the aforementioned antioxidants and bioactive compounds can be degraded during this process.

3.2. Response surface analysis and optimization of phenolics extraction by UAE

The responses (TPC, TFC and AA) corresponding to the CCD matrix for the performed experimental design are given in Table 3. The quadratic default model, Eq. (2), with 10 coefficients has been fitted to each of the response variables. The R-squared statistic indicates that the model as fitted explains 97.32%, 81.84% and 89.78% of the variability in TPC, TFC and AA, respectively.

Analysis of variance (ANOVA) and the values of coefficients of Eq. (2) are shown in Table 4. The significance of each coefficient was determined using the F-ratio and p-value. A large F-ratio and a small p-value imply a more significant effect on the corresponding response variable (Yolmeh et al., 2014). In this case, 4, 2 and 1 coefficients of the quadratic polynomial model of Eq. (2) have p-values less than 0.05 for TPC, TFC and AA, respectively, indicating that they are significantly different from zero at the 95% confidence level. F-ratios indicate that,

Table 4
Analysis of variance (ANOVA) of the regression coefficients for olive pomace phenolic extraction in ultrasonic homogenizer (Time = X_1, S:S ratio = X_2, Amplitude = X_3) of the quadratic Eq. (2) for responses (TPC, TFC and AA).

Source	Total phenolic content (TPC)			Total flavonoid content (TFC)			Antioxidant activity (AA)		
	Regression coefficients	F-ratio	p-value	Regression coefficients	F-ratio	p-value	Regression coefficients	F-ratio	p-value
a_0	17.6842	–	–	2.28613	–	–	1.29098	–	–
a_1	0.157999	0.01	0.9376	0.106996	0.31	0.5989	−0.0527064	0.08	0.7888
a_2	−0.899188	160.91	0.0000	−0.00650216	7.31	0.0354	0.0123156	44.02	0.0006
a_3	−0.259476	31.79	0.0013	−0.0704034	13.28	0.0108	−0.0209026	0.02	0.8932
a_{11}	−0.0578879	4.17	0.0872	−0.0168642	2.79	0.1456	0.00349246	2.58	0.1590
a_{12}	0.00300781	0.14	0.7243	−0.00015625	0.00	0.9587	0.000792969	1.62	0.2505
a_{13}	0.0168438	6.70	0.0413	0.003625	2.45	0.1686	0.000084375	0.03	0.8712
a_{22}	0.0245124	11.96	0.0135	0.000315194	0.02	0.9046	−0.00126751	5.45	0.0583
a_{23}	−0.00254687	0.61	0.4636	−0.0009375	0.66	0.4492	−0.0000484375	0.04	0.8524
a_{33}	0.00533793	1.39	0.2838	0.00150172	0.87	0.3881	0.000353793	1.04	0.3480

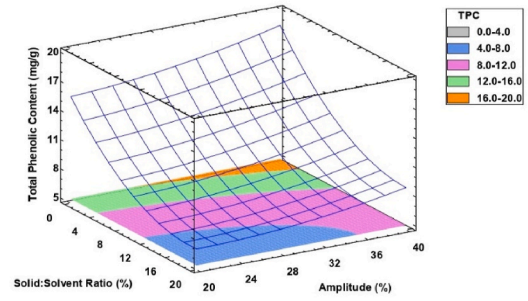

(a)

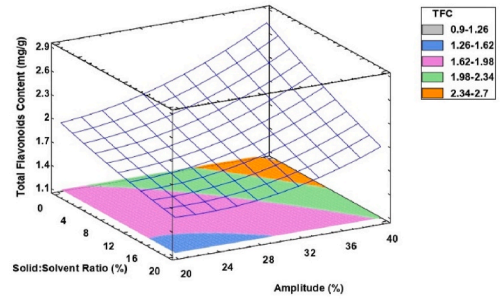

(b)

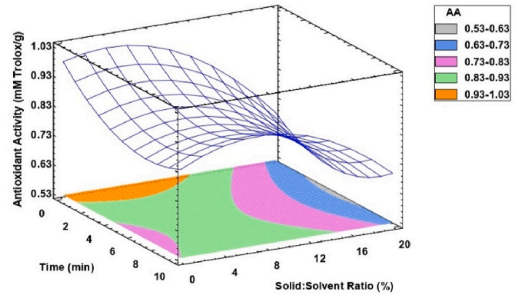

(c)

Fig. 1. Response surface plots of interactions between input factors (X_1, X_2, X_3) and responses (Y_1–Y_3) in ultrasound-assisted phenolics extraction from olive pomace. (a) Interaction of S:S ratio (X_2) and amplitude (X_3) with TPC (Y_1) at central point of time (X_1); (b) Interaction of S:S ratio (X_2) and amplitude (X_3) with TFC (Y_2) at central point of time (X_1); (c) Interaction of time (X_1) and S:S ratio (X_2) with AA (Y_3) at central point of amplitude (X_3).

for the range of studied variables, S:S ratio has stronger influence on TPC and AA, while amplitude has the strongest influence on TFC.

Surface response plots of the quadratic polynomial model were generated by varying two of significant input variables within the experimental range, while holding the third one constant at the central point. Fig. 1a was generated by varying S:S ratio (X_2) and amplitude (X_3), showing their effect on TPC (Y_1) while holding time (X_1) in central point. It is observed that, regardless of ultrasound amplitude, an increase of S:S ratio causes a continuous decrease in TPC which is not favorable. The interaction of S:S ratio (X_2) and amplitude (X_3) and their effect on TFC (Y_2) while holding time (X_1) constant in central point can be observed in Fig. 1b. This figure shows that low values of the S:S ratio (X_2) and high amplitude (X_3) favor obtaining extracts rich in TFC. Fig. 1c shows the interaction between time (X_1) and S:S ratio (X_2) and their effect on AA (Y_3) while holding amplitude (X_3) constant at the central point. It can be observed that S:S ratio has a considerably more significant effect on AA at low S:S ratios, increasing time causes a slight decrease in AA, while at higher S:S ratios there is no significant effect on AA with increasing time.

Numerical optimization was carried out through Design Expert software, using desirability function method. The optimal conditions for the phenolic extraction process used in this work were those leading to highest TPC, TFC and AA. It was predicted that the maximum desirability (94.98%) would be reached for the following operating conditions: time = 9.8 min, amplitude = 40% and S:S ratio = 4% (w/v). The predicted responses for the optimal input factors are 14.95 mg GAE/g, 2.54 mg QE/g and 0.92 mmol Trolox/g for TPC, TFC and AA, respectively.

Regarding the observed responses shown in Table 3, most desirable results were obtained from run 1 (time: 10 min, amplitude: 40%, S:S ratio: 4% (w/v)), with 14.70 mg GAE/g, 2.48 mg QE/g and 0.924 mmol Trolox/g for TPC, TFC and AA, respectively. This proves that experimental results are completely in accordance with the responses predicted by design software.

In a similar study, Goldsmith et al. (2018) used UAE technology for the extraction of phenolic compounds from olive pomace using water as extraction solvent. Optimal conditions were developed using RSM with power, time and sample-to-solvent ratio as input variable factors. The optimal conditions for the extraction of phenolic compounds with high antioxidant activity were 2 g of dried pomace per 100 mL of water at 250 W power for 75 min. Mojerlou and Elhamirad (2018) published a very interesting work in which optimal UAE conditions for olive cake extract through response surface methodology were found at extraction temperature of 56 °C, extraction time of 3 min, duty cycle of 0.6 s, and S:S ratio of 3.6%, obtaining a TPC of 4.04 mg/g and 68.9% of AA.

Ultrasound-assisted extraction was also used for the recovery of antioxidants from extracted olive pomace (EOP). Using ethanol-water solutions as solvent and a 5% w/v S:S ratio, Martínez-Patiño et al. (2019) determined by RSM the following optimal conditions for UAE: 43.2% ethanol concentration, 70% ultrasound amplitude, and 15 min

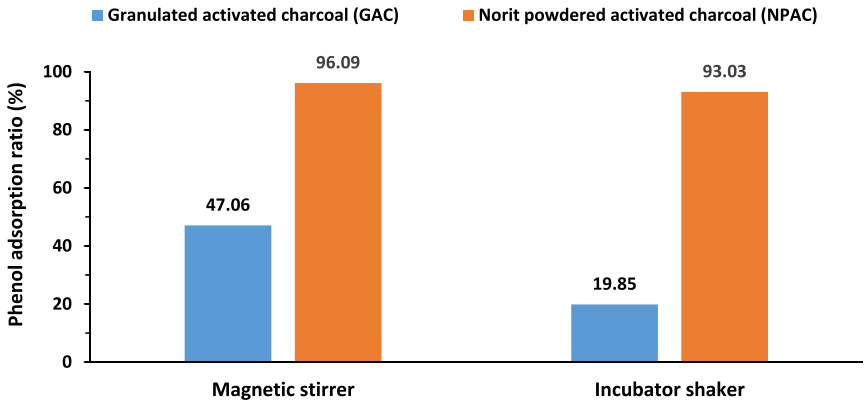

Fig. 2. Phenol adsorption ratio using activated charcoals (50 g/L).

extraction time, yielding an optimal extract with a TPC of 57.5 mg/g and 56.7 mg/g of AA. Contreras et al. (2021) used an ultrasonic bath to perform the UAE from EOP with 47.53% ethanol-water solution as solvent and a S:S ratio of 6%, obtaining a final extract with a TPC of 44.5 mg/g and 0.25 mmol/g of AA after 50 min extraction time.

Conventional extraction processes have several drawbacks mainly related to the use of harmful organic solvents, high energy costs and the degradation of compounds of interest due to high temperatures. Therefore, in recent years concepts such as "green chemistry" and "eco extraction" have emerged (Chemat et al., 2012; Jacotet-Navarro et al., 2015; Rombaut et al., 2014). Even in UAE, it is necessary to avoid the use of high temperatures that can degrade the compounds of interest to be extracted. In similar studies, factors such as temperature or light can induce a degradation of rosemary antioxidants, causing the conversion of carnosic acid into carnosol (Jacotet-Navarro et al., 2015; Zhang et al., 2012). Besides, ultrasound-induced physical impacts led to the total detexturation of rosemary leaves and favored the extraction of leaf metabolites (Khadhraoui et al., 2018). Mojerlou and Elhamirad (2018) also reported the damaging effects of high temperatures on antioxidant activity of phenolic compounds present in olive cake extracts obtained by UAE.

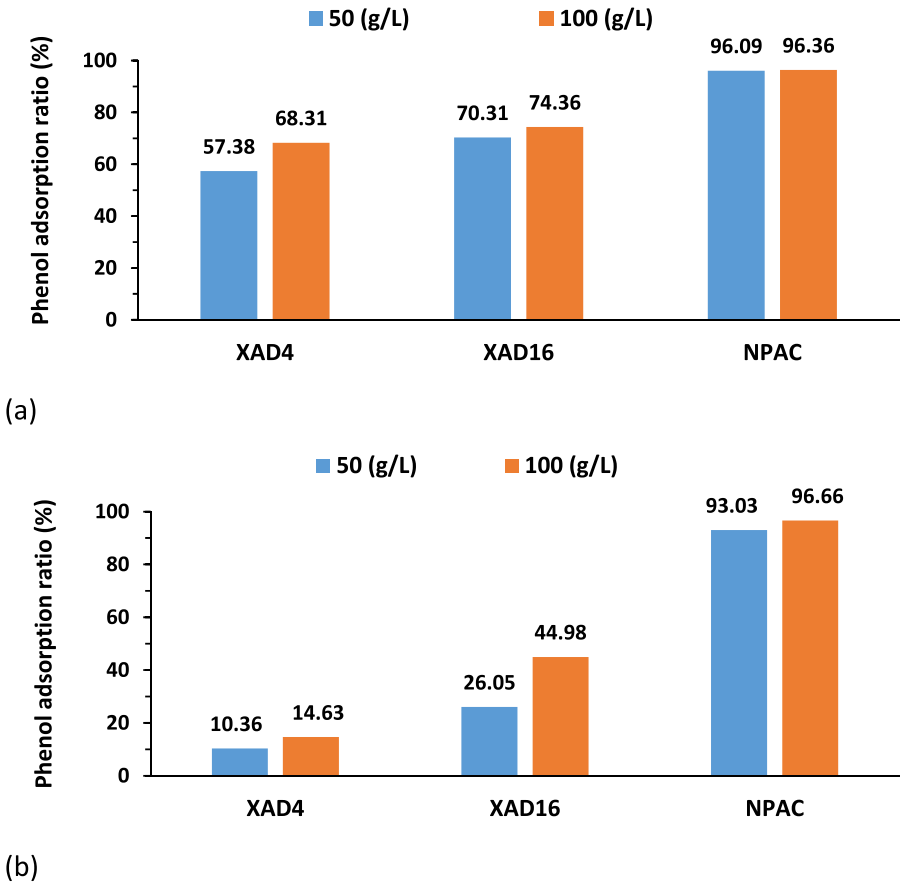

Fig. 3. Phenol adsorption efficiency using several adsorbents and operating devices. (a) Adsorption with magnetic stirrer; (b) Adsorption with incubator shaker.

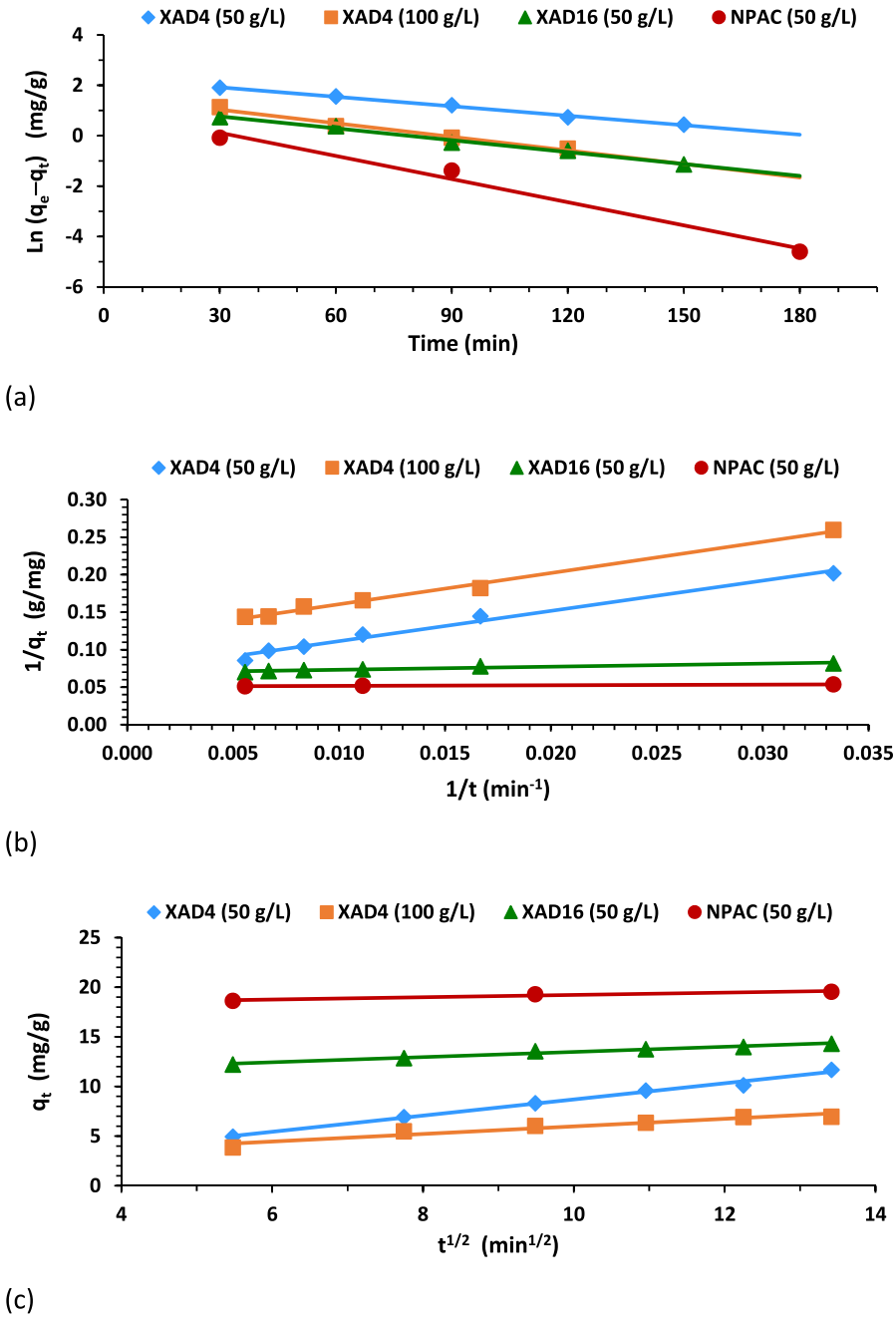

Fig. 4. Phenol adsorption kinetic curves based on different models. (a) Pseudo-first-order kinetic equation; (b) pseudo-second-order kinetic equation; (c) particle diffusion kinetic equation.

3.3. Adsorption-desorption batch experiments

Hydroxytyrosol is not commercially available in large quantities like other food additives. It has been proved by Crea (2002) that pH adjusting of olive mill waste increases its hydroxytyrosol content by up to 400%. Specifically, the addition of acid to the vegetation water up to a pH between 2 and 4, and its subsequent incubation for a period of at least two months, causes that 75% of the oleuropein originally present in the vegetation water becomes in hydroxytyrosol. Besides, adsorption of phenols is strongly dependent on the ionic strength and/or pH value. At acidic pH, the uptake of phenols by different adsorbents is enhanced because phenols are undissociated and dispersion interactions predominate (Kaleh and Geiβen, 2016; Soto et al., 2011). Therefore, in this work, as described in section 2.7, the olive extract, obtained under the aforementioned optimal extraction conditions, was treated by vacuum evaporation to remove ethanol and the remaining extract was acidified to pH 2.8 with HCl (37%) before being used in the adsorption-desorption experiments.

3.3.1. Efficiency of materials and devices in phenol adsorption rates

As it has been already mentioned, preliminary adsorption experiments were performed to select the activated charcoal (AC). Results of adsorption with 50 g AC/L sample are depicted in Fig. 2, where a considerably higher adsorption ratio can be achieved using NPAC regardless of the device used for adsorption process. Therefore, NPAC was selected for the following experiments. This is in accordance with the results of the study performed by Dąbrowski et al. (2005), who concluded that the performance of activated carbon fibers in terms of

Table 5
Analysis of the phenolics adsorption process based on kinetic models using powdered activated charcoal (NPAC) and polymeric resins (XAD4 and XAD16) as adsorbents.

Adsorbent	Adsorbent content (g/L)	q_e exp. (mg/g)	Dynamic equation	Dynamic parameters	R^2
XAD4	50	11.68	$ln(q_e-q_t) = -k_1 t + lnq_e$	$q_e = 9.966$, $k_1 = 0.0125$	0.9955
			$\frac{1}{q_t} = \frac{1}{k_2 q_e^2} \times \frac{1}{t} + \frac{1}{q_e}$	$q_e = 14.085$, $k_2 = 0.0018$	0.9853
			$q_t = k_d t^{1/2} + C$	$k_d = 0.8154$, $C = 0.5373$	0.9923
	100	6.95	$ln(q_e-q_t) = -k_1 t + lnq_e$	$q_e = 4.835$, $k_1 = 0.018$	0.9799
			$\frac{1}{q_t} = \frac{1}{k_2 q_e^2} \times \frac{1}{t} + \frac{1}{q_e}$	$q_e = 8.410$, $k_2 = 0.0050$	0.9930
			$q_t = k_d t^{1/2} + C$	$k_d = 0.3802$, $C = 2.1743$	0.9288
XAD16	50	14.31	$ln(q_e-q_t) = -k_1 t + lnq_e$	$q_e = 3.442$, $k_1 = 0.0157$	0.9915
			$\frac{1}{q_t} = \frac{1}{k_2 q_e^2} \times \frac{1}{t} + \frac{1}{q_e}$	$q_e = 14.493$, $k_2 = 0.0119$	0.9336
			$q_t = k_d t^{1/2} + C$	$k_d = 0.2603$, $C = 10.874$	0.9802
NPAC	50	19.55	$ln(q_e-q_t) = -k_1 t + lnq_e$	$q_e = 2.812$, $k_1 = 0.0306$	0.9845
			$\frac{1}{q_t} = \frac{1}{k_2 q_e^2} \times \frac{1}{t} + \frac{1}{q_e}$	$q_e = 19.724$, $k_2 = 0.0294$	0.9957
			$q_t = k_d t^{1/2} + C$	$k_d = 0.1161$, $C = 18.062$	0.9379

q_e and q_t: amount of phenolic compounds adsorbed at equilibrium and at time t (mg phenols/g adsorbent), respectively; k_1, k_2 and k_d: rate constants for the pseudo-first order, pseudo-second order and particle diffusion kinetic models, respectively; C: constant in the particle diffusion kinetic model; R^2: coefficient of determination.

adsorption rate and selectivity for phenols is significantly higher than that of granular activated carbons.

In order to determine optimal device and operating conditions to perform the adsorption process, a total of 12 adsorption experiments with 50 and 100 g NPAC/L sample were performed using both incubator shaker and magnetic stirrer. After each run, adsorbents were filtered and TPC was determined in the filtrates. Experimental results shown in Fig. 3 demonstrate that there is no significant difference in the performance of the device for phenols adsorption by NPAC, with ratios higher than 90%. Conversely, Fig. 3 shows significant differences for the polymeric resins, for which the use of 100 g resin/L sample and the magnetic stirrer device produces the best conditions for the adsorption of phenols. However, adsorption ratios obtained by incubator shaker are much lower for both resins compared to those with the same operating conditions obtained by magnetic stirrer. Therefore, it can be concluded the efficiency and advantage of using magnetic stirrer for adsorption processes by the application of polymeric resins.

3.3.2. Adsorption kinetics evaluation

The adsorption kinetic curves of XAD4, XAD16 and NPAC are depicted in Fig. 4. In order to elucidate the adsorption mechanisms, pseudo-first-order, pseudo-second-order and particle diffusion kinetic models, described by Eqs. (7)–(9), were tested (Rudzinski and Plazinski, 2008; Yang et al., 2016). The pseudo-first-order model is generally applicable over the initial stage of an adsorption process, while the pseudo-second-order model assumes that the rate-limiting step is chemisorption and predicts the behavior over the whole range of adsorption. Moreover, the particle diffusion kinetic model assumes physical adsorption controlled by diffusion inside particles (Duran et al., 2011; Yang et al., 2016). It was observed that equilibrium adsorption was achieved before 30 min for the experiments with 100 g/L of NPAC and XAD16, so that the kinetics of these experiments could not be evaluated, therefore they are not included in Table 5 nor in Fig. 4. As shown in Table 5, the highest linear correlation coefficients attribute a kinetic model of pseudo-second order for phenolic adsorption with 50 g/L of NPAC and 100 g/L of XAD4; however, pseudo-first order kinetic model would be more appropriate for experiments with 50 g/L of XAD4 and XAD16. Furthermore, in line with other works (Wang et al., 2017; Yang et al., 2016), a pseudo-second order kinetic model for adsorption with XAD4 and XAD16 polymeric resins is reinforced by observing that the equilibrium contents, q_e, calculated as model parameters, are very close to the experimental values, as shown in Table 5.

3.3.3. Phenol selectivity evaluation of adsorption and desorption experiments

A comparative study of the three adsorbents (XAD4, XAD16 and NPAC) with 50 and 100 g/L content for each one, in terms of total phenols recovery and its selectivity for isolation of individual

Table 6
Phenolic content in olive pomace extract and in filtrates of adsorption-desorption experiments. Adsorption and desorption ratios are calculated by Eqs. (4) and (5), respectively, being C_0 the concentration corresponding to the acidified olive pomace extract after evaporation of ethanol.

Stage	Description	Total phenols (mg/L)	Ratio (%)	Hydroxytyrosol (mg/L)	Ratio (%)	Tyrosol (mg/L)	Ratio (%)	Oleuropein (mg/L)	Ratio (%)
Olive pomace extract	Initial	415.65 ± 9.98	–	14.51 ± 4.17	–	4.58 ± 2.35	–	7.85 ± 0.26	–
	After acidification	497.41 ± 4.16	–	17.99 ± 9.64	–	8.9 ± 4.87	–	9.5 ± 1.28	–
	After ethanol evaporation (C_0)	1017.46 ± 0.54	–	82.03 ± 12.44	–	37.81 ± 9.49	–	16.52 ± 0.94	–
Adsorption	XAD4 (50 g/L)	433.62 ± 15.77	57.38	56.66 ± 0.06	30.93	17.02 ± 0.52	54.99	0	100.00
	XAD4 (100 g/L)	322.46 ± 10.88	68.31	49.36 ± 0.86	39.83	11.51 ± 1.51	69.56	0	100.00
	XAD16 (50 g/L)	302.08 ± 8.16	70.31	35.82 ± 2.0	56.33	10.26 ± 1.89	72.86	0	100.00
	XAD16 (100 g/L)	260.92 ± 2.18	74.36	49.83 ± 0.96	39.25	11.8 ± 0.62	68.79	0	100.00
	NPAC (50 g/L)	39.77 ± 0.54	96.09	7.21 ± 0.13	91.21	1.2 ± 0	96.83	0	100.00
	NPAC (100 g/L)	37.08 ± 1.09	96.36	7.23 ± 0.95	91.19	0.2 ± 0	99.47	0	100.00
Desorption	XAD4 (50 g/L)	566.24 ± 23.29	96.99	6.64 ± 2.40	26.17	1.96 ± 0.03	9.43	5.51 ± 0.01	33.35
	XAD4 (100 g/L)	556.53 ± 19.55	80.08	9.85 ± 2.17	30.15	4.17 ± 2.06	15.84	4.11 ± 0.01	24.88
	XAD16 (50 g/L)	571.53 ± 5.82	79.89	7.12 ± 1.14	15.41	2.43 ± 0.98	8.82	1.04 ± 0.01	6.30
	XAD16 (100 g/L)	531.82 ± 16.22	70.30	11.58 ± 2.41	35.96	4.23 ± 0.06	16.26	5.30 ± 2.25	32.08
	NPAC (50 g/L)	228.88 ± 7.90	23.41	7.34 ± 0.91	9.81	3.51 ± 1.25	9.59	1.36 ± 1.14	8.23
	NPAC (100 g/L)	171.24 ± 2.91	17.47	7.57 ± 3.40	10.12	3.43 ± 0.76	9.12	1.39 ± 0.55	8.41

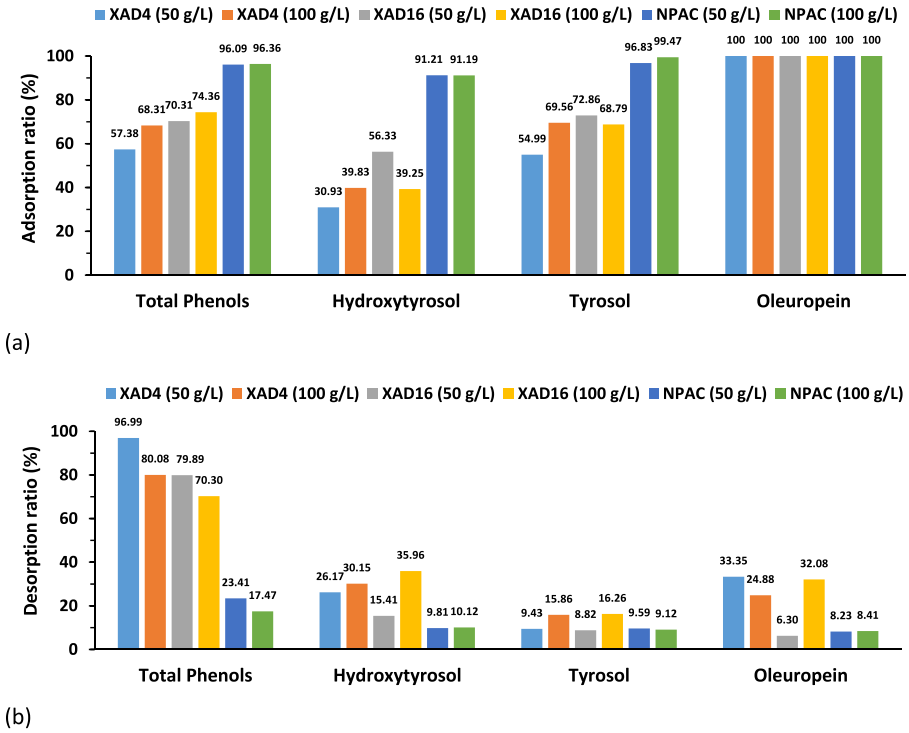

Fig. 5. Experimental comparison of phenol adsorption (a) and desorption (b) ratios between the adsorbents.

compounds (specifically hydroxytyrosol, tyrosol and oleuropein) was made with the same pattern. Mean values of these compounds in filtrates after adsorption and desorption stages, together with those of the initial sample of the olive extract, are shown in Table 6. Adsorption and desorption ratios calculated by Eqs. (4) and (5), respectively, are depicted in Fig. 5.

Fig. 5a shows that NPAC has the higher adsorption ratios, over 91% for all phenolic compounds, regardless of the adsorbent input content (50 or 100 g/L). This is in accordance with the study performed by Fava et al. (2017) for the recovery up to 80% of polyphenols from OMWW. Furthermore, XAD16 also shows a high adsorption ratio of total phenols with 74.36% and 70.31% for contents of 100 and 50 g/L, respectively, which are higher than those obtained with XAD4 (68.31% and 57.38%, respectively). In general, the XAD16 and XAD4 resins show a higher adsorption ratio for tyrosol than for hydroxytyrosol. Successful adsorption results for XAD16 resin have been published in several studies (Frascari et al., 2019; Pinelli et al., 2016; Zagklis and Paraskeva, 2018). Regarding oleuropein isolation, all three types of adsorbents show excellent efficiency with 100% adsorption ratios.

Experimental evaluation of desorption ratios is presented in Fig. 5b. As it is mentioned earlier, ethanol was used as desorption solvent. In this study, desorption ratio correlation of total phenol and individual phenolic compounds was not completely satisfactory. XAD4 with 50 g/L content proved highest desorption ratio of total phenols with 96.99% but showed 26.17%, 9.43% and 33.35% desorption ratios for hydroxytyrosol, tyrosol and oleuropein, respectively. However, in the experiment with 100 g/L of XAD4, lower desorption values were obtained for total phenols (80.08%), but higher for the individual phenols (30.15%, 15.86%, and 24.88% for hydroxytyrosol, tyrosol and oleuropein, respectively). Similar trend was observed by using XAD16 resin: XAD16 with 50 g/L content had almost 13% better desorption ratio of total phenols compared to the same resin with 100 g/L content. However, XAD16 with 100 g/L content showed significantly higher results for desorbing individual phenolic compounds compared to XAD16 with 50 g/L content.

The desorption recovery factors, calculated by Eq. (6), indicate that the best results were obtained by using the XAD16 resin with 100 g/L content, for which total recoveries were 52.27% of TPC, 14.12% of hydroxytyrosol, 11.19% of tyrosol and 32.08% of oleuropein (see Table 7). Such results were higher than those obtained for 50 g/L XAD16: 8.68% of hydroxytyrosol, 6.43% of tyrosol and 6.29% of oleuropein, despite the fact that the recovery of TPC was slightly higher than 56.17%. Regarding NPAC, TPC recoveries were 22.50% and 16.83% for contents of 50 and 100 g/L, respectively, which are considerably lower than those obtained with the polymeric resins.

Supplementary desorption kinetic experiments were performed in order to check the equilibrium conditions in the explanation of the results. In these experiments, aliquots (1.0 mL) of supernatant of the filtered samples were taken at the time points of 30, 60, 90 and 120 min and the TPC in the solutions was measured. Results are depicted in Fig. 6. It can be observed that for all of experimental series, the majority of phenol recovery occur in the first 30 min of desorption process and then they reach the equilibrium. This corroborates that the results of Table 6, which were taken after 2 h of contact, are equilibrium values.

The most important advantage of ethanol as a desorption solvent is its high volatility and ease of use in energy efficient vacuum evaporators: the final concentration of valuable phenolic compounds will be significantly increased with economic advantages of paramount importance at industrial scale. In this way, Zagklis et al. (2015) recovered 74% of the initial amount of hydroxytyrosol by vacuum evaporation of ethanol until reach a volume concentration factor of 5.4.

Additionally, in order to study the possibility of improvements for recovery results, some extra desorption runs were performed using the optimal adsorption series which were NPAC (100 g/L) and XAD16 (100 g/L). For this purpose, another four solvents were considered to be used: acidified ethanol (pH = 2.0), ethanol-water (1:1), ethanol-water (1:1) acidified to pH = 2.3, and acetic acid solution (0.5 M). The desorption recovery results calculated by Eq. (6) are provided in Table 7, along with those previously obtained with ethanol at natural pH (about 7), for comparison purposes. With respect to 100 g/L XAD16, it can be observed that acidified ethanol (pH = 2.0) improves the recovery of TPC (64.35%) with respect to ethanol at natural pH (52.27%). The highest

Table 7
Adsorption-desorption experiments with XAD16 and NPAC adsorbents and 100 g/L content using different desorption solvents. Values correspond to the filtrate concentration in desorption stage and recovery calculated by Eq. (6).

Solvent	Responses	XAD16 (100 g/L)		NPAC (100 g/L)	
		Mean value (mg/L)	Desorption recovery (%)	Mean value (mg/L)	Desorption recovery (%)
Ethanol (100%, pH natural ≈ 7)	TPC	531.82 ± 16.22	52.27	171.24 ± 2.91	16.83
	HT	11.58 ± 2.41	14.12	7.57 ± 3.40	9.23
	TY	4.23 ± 0.06	11.19	3.43 ± 0.76	9.07
	OLE	5.30 ± 2.25	32.08	1.39 ± 0.55	8.41
Ethanol (100%, pH = 2.0)	TPC	654.76 ± 35.36	64.35	175.35 ± 7.90	17.23
	HT	5.40 ± 1.70	6.58	1.07 ± 0.14	1.30
	TY	3.26 ± 0.11	8.62	3.30 ± 0.33	8.73
	OLE	0.75 ± 0.02	4.54	–	0
Ethanol-water (1:1 v/v, pH = 4.1)	TPC	568.38 ± 0.01	55.86	122.87 ± 5.50	12.08
	HT	8.14 ± 0.67	9.92	3.25 ± 0.4	3.96
	TY	2.63 ± 0.2	6.96	4.13 ± 2.21	10.92
	OLE	–	0	–	0
Ethanol-water (1:1 v/v, pH = 2.3)	TPC	586.53 ± 19.55	57.65	122.71 ± 2.50	12.06
	HT	15.81 ± 2.02	19.27	3.14 ± 0.36	3.83
	TY	17.29 ± 2.09	45.73	7.98 ± 2.30	21.11
	OLE	–	0	–	
Acetic acid (0.5 M)	TPC	92.68 ± 2.61	9.11	13.23 ± 0.8	1.30
	HT	20.12 ± 0.35	24.53	4.33 ± 0.5	5.28
	TY	1.77 ± 0.51	4.68	–	0
	OLE	–	0	–	0

TPC: Total phenolic content; HT: Hydroxytyrosol; TY: Tyrosol; OLE: Oleuropein.

recovery of hydroxytyrosol (24.53%) was obtained with acetic acid 0.5 M, although the TPC recovery was only 9.11% with this solvent. In general, the optimal results were obtained by using the acidified ethanol-water solution (1:1 v/v, pH = 2.3) yielding recoveries of 19.23% for hydroxytyrosol, 57.65% for TPC and 45.73% for tyrosol. However, no oleuropein was identified in this solvent after desorption. NPAC did not prove any significant improvements in the additional desorption experiments, except for tyrosol recovery with acidified ethanol-water (pH = 2.0) solution (21.11%) which was considerably higher than the obtained with the other solvents.

In addition, according to Table 7, acetic acid (0.5 M) did not show promising results for TPC desorption, but hydroxytyrosol was 24.53% of the desorbed phenolic compounds. This indicates a considerable selectivity and high purification ability when using acetic acid as a desorption solvent for hydroxytyrosol recovery.

It should be noted that the optimal olive extract after phenolic extraction was vacuum concentrated with a factor of 2, while the corresponding mean values of the desorption stage presented in Tables 6 and 7 were obtained using half of solvent volume, compared to the volume of the initial extract before vacuum concentration. The use of small volumes of solvent is interesting from an economic and environmental point of view. Nevertheless, more studies should be carried out on solvent selection for the NPAC desorption stage to improve the phenolics recovery, taking advantage of its excellent adsorption capacity. Furthermore, different adsorbents could be investigated to improve the selective isolation of hydroxytyrosol, tyrosol and oleuropein.

As previously stated in the study of Ahmed et al. (2019), the future perspectives of the olive oil industry should be based on a biorefinery framework using olive mill solid and liquid waste streams as feed to obtain high added value products, such as antioxidants, biochemicals, catalyzers and biofuels. Several biotechnological production processes should be developed and implemented to achieve this goal, and the products obtained could enhance the economic viability of this industry and reduce its footprints. Furthermore, the high potential of the olive oil industry to be transformed into biorefineries would also constitute a solution for the treatment of these waste streams (Ahmed et al., 2019) complying with the most stringent environmental policies, in a circular economy context.

Life cycle assessment (LCA), energy and exergy are the most common methods used for evaluation of sustainability features in biorefineries, especially for the quantitative and qualitative assessment of biofuel production (Dadak et al., 2016), and thus should help the advance of this industry (Rosen, 2018).

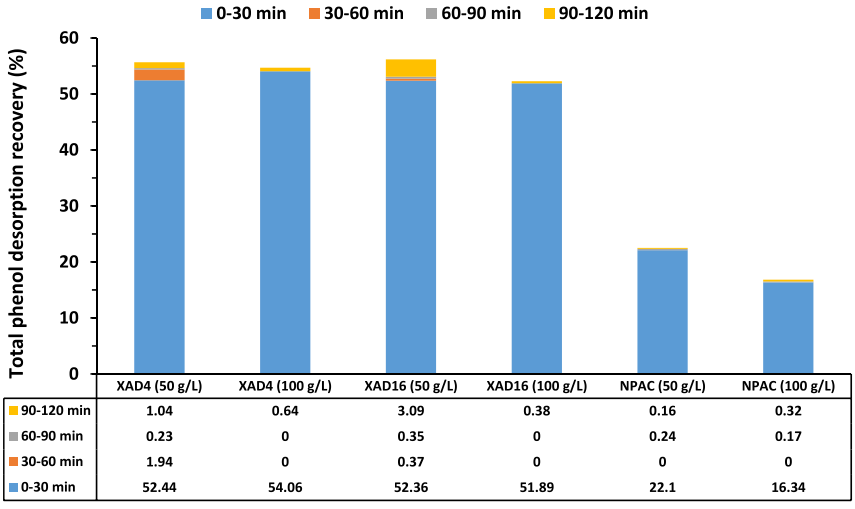

Fig. 6. Evaluation of total phenol desorption recovery in time periods.

4. Conclusions and future research needs

This study aims to develop a technology for actual treatment of olive mill solid residue. Oil fraction extracted from Soxhlet defatting process is essentially rich in monounsaturated fatty acids, mainly oleic acid. The defatted olive pomace can be further processed for biophenols recovery. A liquid fraction rich in hydroxytyrosol and tyrosol, highly profitable due to its antioxidant properties, was obtained by ultrasound-assisted extraction using 50% v/v ethanol-water as solvent, followed by adsorption-desorption stages with the XAD16 polymeric resin and acidified ethanol-water (1:1 v/v) at pH = 2.3. This efficient treatment could be proposed as a competitive method to upgrade olive oil production plants, reducing waste generation and obtaining by-products with high added market value.

The future needs of the olive oil industry should be based on a biorefinery framework using olive mill waste streams as feed to obtain high added value products. The evaluation of its sustainability features should still be investigated using advanced tools such as life cycle assessment, energy and exergy, with the main goals of enhance the economic viability of this industry, reduce its footprints and comply with the most stringent environmental policies in a circular economy context.

CRediT authorship contribution statement

S. Mehdi Niknam: Investigation, Validation, Formal analysis, Writing – original draft. **Mansoore Kashaninejad:** Investigation. **Isabel Escudero:** Conceptualization, Methodology, Project administration, Writing – review & editing. **M. Teresa Sanz:** Funding acquisition, Resources, Validation. **Sagrario Beltrán:** Funding acquisition, Resources, Validation. **José M. Benito:** Supervision, Conceptualization, Formal analysis, Methodology, Writing – review & editing.

Declaration of competing interest

The authors declare that they have no known competing financial interests or personal relationships that could have appeared to influence the work reported in this paper.

Acknowledgments

This work was supported by the Spanish Agencia Estatal de Investigación [grant number PID2019-104950RB-I00/AEI/10.13039/501100011033] and the Junta de Castilla y León (JCyL) and the European Regional Development Fund (ERDF) [grant numbers BU301P18 and BU050P20].

References

Ahmed, P.M., Fernández, P.M., de Figueroa, L.I.C., Pajot, H.F., 2019. Exploitation alternatives of olive mill wastewater: production of value-added compounds useful for industry and agriculture. Biofuel Res. J. 22, 980–994. https://doi.org/10.18331/BRJ2019.6.2.4.

Akay, F., Kazan, A., Celiktas, M.S., Yesil-Celiktas, O., 2015. A holistic engineering approach for utilization of olive pomace. J. Supercrit. Fluids 99, 1–7. https://doi.org/10.1016/j.supflu.2015.01.025.

Al Juhaimi, F., Özcan, M.M., Uslu, N., Ghafoor, K., 2018. The effect of drying temperatures on antioxidant activity, phenolic compounds, fatty acid composition and tocopherol contents in citrus seed and oils. J. Food Sci. Technol. 55, 190–197. https://doi.org/10.1007/s13197-017-2895-y.

Allaf, T., Tomao, V., Ruiz, K., Chemat, F., 2013. Instant controlled pressure drop technology and ultrasound assisted extraction for sequential extraction of essential oil and antioxidants. Ultrason. Sonochem. 20, 239–246. https://doi.org/10.1016/j.ultsonch.2012.05.013.

Allalout, A., Krichène, D., Methenni, K., Taamalli, A., Oueslati, I., Daoud, D., Zarrouk, M., 2009. Characterization of virgin olive oil from Super Intensive Spanish and Greek varieties grown in northern Tunisia. Sci. Hortic. 120, 77–83. https://doi.org/10.1016/j.scienta.2008.10.006.

Alu'datt, M.H., Alli, I., Ereifej, K., Alhamad, M., Al-Tawaha, A.R., Rababah, T., 2010. Optimisation, characterisation and quantification of phenolic compounds in olive cake. Food Chem. 123, 117–122. https://doi.org/10.1016/j.foodchem.2010.04.011.

Antónia Nunes, M., Costa, A.S.G., Bessada, S., Santos, J., Puga, H., Alves, R.C., Freitas, V., Oliveira, M.B.P.P., 2018. Olive pomace as a valuable source of bioactive compounds: a study regarding its lipid- and water-soluble components. Sci. Total Environ. 644, 229–236. https://doi.org/10.1016/j.scitotenv.2018.06.350.

AOAC, 1995. AOAC Official Method 991.39. Fatty Acids in Encapsulated Fish Oils and Fish Oil Methyl and Ethyl Esters. Gas Chromatographic Method.

Azmir, J., Zaidul, I.S.M., Rahman, M.M., Sharif, K.M., Mohamed, A., Sahena, F., Jahurul, M.H.A., Ghafoor, K., Norulaini, N.A.N., Omar, A.K.M., 2013. Techniques for extraction of bioactive compounds from plant materials: a review. J. Food Eng. 117, 426–436. https://doi.org/10.1016/j.jfoodeng.2013.01.014.

Chang, C.-C., Yang, M.-H., Wen, H.-M., Chern, J.-C., 2002. Estimation of total flavonoid content in propolis by two complementary colorimetric methods. J. Food Drug Anal. 10, 178–182. https://doi.org/10.38212/2224-6614.2748.

Chemat, F., Tomao, V., Virot, M., 2008. Ultrasound-assisted extraction in food analysis. In: Otleş, S. (Ed.), Handbook of Food Analysis Instruments. CRC Press, Boca Raton, pp. 85–103. https://doi.org/10.1201/9781420045673.

Chemat, F., Vian, M.A., Cravotto, G., 2012. Green extraction of natural products: concept and principles. Int. J. Mol. Sci. 13, 8615–8627. https://doi.org/10.3390/ijms13078615.

Chemat, F., Rombaut, N., Meullemiestre, A., Turk, M., Perino, S., Fabiano-Tixier, A.-S., Abert-Vian, M., 2017a. Review of green food processing techniques. Preservation, transformation, and extraction. Innovat. Food Sci. Emerg. Technol. 41, 357–377. https://doi.org/10.1016/j.ifset.2017.04.016.

Chemat, F., Rombaut, N., Sicaire, A.-G., Meullemiestre, A., Fabiano-Tixier, A.-S., Abert-Vian, M., 2017b. Ultrasound assisted extraction of food and natural products. Mechanisms, techniques, combinations, protocols and applications. Rev. Ultrason. Sonochem. 34, 540–560. https://doi.org/10.1016/j.ultsonch.2016.06.035.

Chemat, F., Abert Vian, M., Fabiano-Tixier, A.-S., Nutrizio, M., Jambrak, A.R., Munekata, P.E.S., Lorenzo, J.M., Barba, F.J., Binello, A., Cravotto, G., 2020. A review of sustainable and intensified techniques for extraction of food and natural products. Green Chem. 22, 2325–2353. https://doi.org/10.1039/c9gc03878g.

Codex Alimentarius, 2013. Standard for Olive Oils and Olive Pomace Oils (CXS 33-1981). FAO-WHO.

Contreras, M.d.M., Gómez-Cruz, I., Romero, I., Castro, E., 2021. Olive pomace-derived biomasses fractionation through a two-step extraction based on the use of ultrasounds: chemical characteristics. Foods 10, 111. https://doi.org/10.3390/foods10010111.

Crea, R., 2002. Method of Obtaining a Hydroxytyrosol-Rich Composition from Vegetation Water. Patent WO 02/18310 A1.

Dadak, A., Aghbashlo, M., Tabatabaei, M., Najafpour, G., Younesi, H., 2016. Sustainability assessment of photobiological hydrogen production using anaerobic bacteria (*Rhodospirillum rubrum*) via exergy concept: effect of substrate concentrations. Environ. Prog. Sustain. Energy 35, 1166–1176. https://doi.org/10.1002/ep.12296.

Dąbrowski, A., Podkościelny, P., Hubicki, Z., Barczak, M., 2005. Adsorption of phenolic compounds by activated carbon - a critical review. Chemosphere 58, 1049–1070. https://doi.org/10.1016/j.chemosphere.2004.09.067.

Duran, C., Ozdes, D., Gundogdu, A., Senturk, H.B., 2011. Kinetics and isotherm analysis of basic dyes adsorption onto almond shell (*Prunus dulcis*) as a low cost adsorbent. J. Chem. Eng. Data 56, 2136–2147. https://doi.org/10.1021/je101204j.

Espín, J.C., Soler-Rivas, C., Cantos, E., Tomás-Barberán, F.A., Wichers, H.J., 2001. Synthesis of the antioxidant hydroxytyrosol using tyrosinase as biocatalyst. J. Agric. Food Chem. 49, 1187–1193. https://doi.org/10.1021/jf001258b.

FAOSTAT. Food and Agriculture Organization of the United Nations, Statistics Division. http://www.fao.org/faostat accessed 11 June 2021.

Fava, G., Di Mauro, M.D., Spampinato, M., Biondi, D., Gambera, G., Centonze, G., Maggiore, R., D'Antona, N., 2017. Hydroxytyrosol recovery from olive mill wastewater: process optimization and development of a pilot plant. Clean 45 (4), 1600042. https://doi.org/10.1002/clen.201600042.

Frascari, D., Rubertelli, G., Arous, F., Ragini, A., Bresciani, L., Arzu, A., Pinelli, D., 2019. Valorisation of olive mill wastewater by phenolic compounds adsorption: development and application of a procedure for adsorbent selection. Chem. Eng. J. 360, 124–138. https://doi.org/10.1016/j.cej.2018.11.188.

Gebreyohannes, A.Y., Mazzei, R., Giorno, L., 2016. Trends and current practices of olive mill wastewater treatment: application of integrated membrane process and its future perspective. Separ. Purif. Technol. 162, 45–60. https://doi.org/10.1016/j.seppur.2016.02.001.

Ghorbannezhad, P., Bay, A., Yolmeh, M., Yadollahi, R., Moghadam, J.Y., 2016. Optimization of coagulation–flocculation process for medium density fiberboard (MDF) wastewater through response surface methodology. Desalin. Water Treat. 57, 26916–26931. https://doi.org/10.1080/19443994.2016.1170636.

Goldsmith, C.D., Vuong, Q.V., Stathopoulos, C.E., Roach, P.D., Scarlett, C.J., 2018. Ultrasound increases the aqueous extraction of phenolic compounds with high antioxidant activity from olive pomace. LWT - Food Sci. Technol. (Lebensmittel-Wissenschaft -Technol.) 89, 284–290. https://doi.org/10.1016/j.lwt.2017.10.065.

Hoff, J.E., Singleton, K.I., 1977. A method for determination of tannins in foods by means of immobilized protein. J. Food Sci. 42, 1566–1569. https://doi.org/10.1111/j.1365-2621.1977.tb08427.x.

Hu, T., He, X.-W., Jiang, J.-G., Xu, X.-L., 2014. Hydroxytyrosol and its potential therapeutic effects. J. Agric. Food Chem. 62, 1449–1455. https://doi.org/10.1021/jf405820v.

Jacotet-Navarro, M., Rombaut, N., Fabiano-Tixier, A.-S., Danguien, M., Bily, A., Chemat, F., 2015. Ultrasound versus microwave as green processes for extraction of rosmarinic, carnosic and ursolic acids from rosemary. Ultrason. Sonochem. 27, 102–109. https://doi.org/10.1016/j.ultsonch.2015.05.006.

Kaleh, Z., Geißen, S.-U., 2016. Selective isolation of valuable biophenols from olive mill wastewater. J. Environ. Chem. Eng. 4, 373–384. https://doi.org/10.1016/j.jece.2015.11.010.

Kammerer, J., Kammerer, D.R., Jensen, U., Carle, R., 2010. Interaction of apple polyphenols in a multi-compound system upon adsorption onto a food-grade resin. J. Food Eng. 96, 544–554. https://doi.org/10.1016/j.jfoodeng.2009.08.038.

Khadhraoui, B., Turk, M., Fabiano-Tixier, A.S., Petitcolas, E., Robinet, P., Imbert, R., El Maâtaoui, M., Chemat, F., 2018. Histo-cytochemistry and scanning electron microscopy for studying spatial and temporal extraction of metabolites induced by ultrasound. Towards chain detexturation mechanism. Ultrason. Sonochem. 42, 482–492. https://doi.org/10.1016/j.ultsonch.2017.11.029.

Khoufi, S., Hamza, M., Sayadi, S., 2011. Enzymatic hydrolysis of olive wastewater for hydroxytyrosol enrichment. Bioresour. Technol. 102, 9050–9058. https://doi.org/10.1016/j.biortech.2011.07.048.

Lafka, T.-I., Lazou, A.E., Sinanoglou, V.J., Lazos, E.S., 2011. Phenolic and antioxidant potential of olive oil mill wastes. Food Chem. 125, 92–98. https://doi.org/10.1016/j.foodchem.2010.08.041.

Leighton, T.G., 2007. What is ultrasound? Prog. Biophys. Mol. Biol. 93, 3–83. https://doi.org/10.1016/j.pbiomolbio.2006.07.026.

Ma, Y., Ye, X., Hao, Y., Xu, G., Xu, G., Liu, D., 2008. Ultrasound-assisted extraction of hesperidin from Penggan (*Citrus reticulata*) peel. Ultrason. Sonochem. 15, 227–232. https://doi.org/10.1016/j.ultsonch.2007.03.006.

Ma, Y.-Q., Chen, J.-C., Liu, D.-H., Ye, X.-Q., 2009. Simultaneous extraction of phenolic compounds of citrus peel extracts: effect of ultrasound. Ultrason. Sonochem. 16, 57–62. https://doi.org/10.1016/j.ultsonch.2008.04.012.

Manzanares, P., Ruiz, E., Ballesteros, M., Negro, M.J., Gallego, F.J., López-Linares, J.C., Castro, E., 2017. Residual biomass potential in olive tree cultivation and olive oil industry in Spain: valorization proposal in a biorefinery context. Spanish J. Agric. Res. 15, e0206 https://doi.org/10.5424/sjar/2017153-10868.

Martínez-Patiño, J.C., Gómez-Cruz, I., Romero, I., Gullón, B., Ruiz, E., Brnčić, M., Castro, E., 2019. Ultrasound-assisted extraction as a first step in a biorefinery strategy for valorisation of extracted olive pomace. Energies 12, 2679. https://doi.org/10.3390/en12142679.

Misra, N.N., Martynenko, A., Chemat, F., Paniwnyk, L., Barba, F.J., Jambrak, A.R., 2018. Thermodynamics, transport phenomena, and electrochemistry of external field-assisted nonthermal food technologies. Crit. Rev. Food Sci. Nutr. 58, 1832–1863. https://doi.org/10.1080/10408398.2017.1287660.

Mojerlou, Z., Elhamirad, A., 2018. Optimization of ultrasound-assisted extraction (UAE) of phenolic compounds from olive cake. J. Food Sci. Technol. 55, 977–984. https://doi.org/10.1007/s13197-017-3005-x.

Niknam, S.M., Escudero, I., Benito, J.M., 2020. Formulation and preparation of water-in-oil-in-water emulsions loaded with a phenolic-rich inner aqueous phase. Foods 9, 1411. https://doi.org/10.3390/foods9101411.

Orsavova, J., Misurcova, L., Ambrozova, J.V., Vicha, R., Mlcek, J., 2015. Fatty acids composition of vegetable oils and its contribution to dietary energy intake and dependence of cardiovascular mortality on dietary intake of fatty acids. Int. J. Mol. Sci. 16, 12871–12890. https://doi.org/10.3390/ijms160612871.

Parascanu, M.M., Sánchez, P., Soreanu, G., Valverde, J.L., Sánchez-Silva, L., 2018. Environmental assessment of olive pomace valorization through two different thermochemical processes for energy production. J. Clean. Prod. 186, 771–781. https://doi.org/10.1016/j.jclepro.2018.03.169.

Pinelli, D., Molina Bacca, A.E., Kaushik, A., Basu, S., Nocentini, M., Bertin, L., Frascari, D., 2016. Batch and continuous flow adsorption of phenolic compounds from olive mill wastewater: a comparison between nonionic and ion exchange resins. Int. J. Chem. Eng. 9349627. https://doi.org/10.1155/2016/9349627, 2016.

Richard, D., Delgado Núñez, M. de L., Schweich, D., 2009. Adsorption of complex phenolic compounds on active charcoal: adsorption capacity and isotherms. Chem. Eng. J. 148, 1–7. https://doi.org/10.1016/j.cej.2008.07.023.

Rodríguez-Gutiérrez, G., Lama-Muñoz, A., Ruiz-Méndez, M.V., Rubio-Senent, F., Fernández-Bolaños, J., 2012. New olive-pomace oil improved by hydrothermal pretreatments. In: Boskou, D. (Ed.), Olive Oil – Constituents, Quality, Health Properties and Bioconversions. InTech, Rijeka, pp. 249–266. https://doi.org/10.5772/28742.

Rombaut, N., Tixier, A.-S., Bily, A., Chemat, F., 2014. Green extraction processes of natural products as tools for biorefinery. Biofuels Bioprod. Biorefining 8, 530–544. https://doi.org/10.1002/bbb.1486.

Rosen, M.A., 2018. Environmental sustainability tools in the biofuel industry. Biofuel Res. J. 17, 751–752. https://doi.org/10.18331/BRJ2018.5.1.2.

Rudzinski, W., Plazinski, W., 2008. Kinetics of dyes adsorption at the solid-solution interfaces: a theoretical description based on the two-step kinetic model. Environ. Sci. Technol. 42, 2470–2475. https://doi.org/10.1021/es7025278.

Sánchez Moral, P., Ruiz Méndez, M.V., 2006. Production of pomace olive oil. Grasas Aceites 57, 47–55. https://doi.org/10.3989/gya.2006.v57.i1.21.

Santos, S.C.R.V.L., Guiné, R.P.F., Barros, A., 2014. Effect of drying temperatures on the phenolic composition and antioxidant activity of pears of Rocha variety (*Pyrus communis* L.). Food Measure 8, 105–112. https://doi.org/10.1007/s11694-014-9170-y.

Shen, Q., Zhang, B., Xu, R., Wang, Y., Ding, X., Li, P., 2010. Antioxidant activity in vitro of the selenium-contained protein from the Se-enriched *Bifidobacterium animalis* 01. Anaerobe 16, 380–386. https://doi.org/10.1016/j.anaerobe.2010.06.006.

Soto, M.L., Moure, A., Domínguez, H., Parajó, J.C., 2011. Recovery, concentration and purification of phenolic compounds by adsorption: a review. J. Food Eng. 105, 1–27. https://doi.org/10.1016/j.jfoodeng.2011.02.010.

Suárez, M., Romero, M.-P., Ramo, T., Macià, A., Motilva, M.-J., 2009. Methods for preparing phenolic extracts from olive cake for potential application as food antioxidants. J. Agric. Food Chem. 57, 1463–1472. https://doi.org/10.1021/jf8032254.

Sun, Y., Liu, D., Chen, J., Ye, X., Yu, D., 2011. Effects of different factors of ultrasound treatment on the extraction yield of the all-*trans*-β-carotene from citrus peels. Ultrason. Sonochem. 18, 243–249. https://doi.org/10.1016/j.ultsonch.2010.05.014.

Tsagaraki, E., Lazarides, H., 2012. Fouling analysis and performance of tubular ultrafiltration on pretreated olive mill waste water. Food Bioprocess Technol. 5, 584–592. https://doi.org/10.1007/s11947-010-0326-4.

Uribe, E., Lemus-Mondaca, R., Vega-Gálvez, A., López, L.A., Pereira, K., López, J., Ah-Hen, K., Di Scala, K., 2013. Quality characterization of waste olive cake during hot air drying: nutritional aspects and antioxidant activity. Food Bioprocess Technol. 6, 1207–1217. https://doi.org/10.1007/s11947-012-0802-0.

Uribe, E., Lemus-Mondaca, R., Vega-Gálvez, A., Zamorano, M., Quispe-Fuentes, I., Pasten, A., Di Scala, K., 2014. Influence of process temperature on drying kinetics, physicochemical properties and antioxidant capacity of the olive-waste cake. Food Chem. 147, 170–176. https://doi.org/10.1016/j.foodchem.2013.09.121.

Wang, Z., Wang, C., Yuan, J., Zhang, C., 2017. Adsorption characteristics of adsorbent resins and antioxidant capacity for enrichment of phenolics from two-phase olive waste. J. Chromatogr. B 1040, 38–46. https://doi.org/10.1016/j.jchromb.2016.11.023.

Yang, Q., Zhao, M., Lin, L., 2016. Adsorption and desorption characteristics of adlay bran free phenolics on macroporous resins. Food Chem. 194, 900–907. https://doi.org/10.1016/j.foodchem.2015.08.070.

Yangui, A., Abderrabba, M., Sayari, A., 2017a. Amine-modified mesoporous silica for quantitative adsorption and release of hydroxytyrosol and other phenolic compounds from olive mill wastewater. J. Taiwan Inst. Chem. Eng. 70, 111–118. https://doi.org/10.1016/j.jtice.2016.10.053.

Yangui, A., Njimou, J.R., Cicci, A., Bravi, M., Abderrabba, M., Chianese, A., 2017b. Competitive adsorption, selectivity and separation of valuable hydroxytyrosol and toxic phenol from olive mill wastewater. J. Environ. Chem. Eng. 5, 3581–3589. https://doi.org/10.1016/j.jece.2017.06.037.

Yolmeh, M., Habibi Najafi, M.B., Farhoosh, R., 2014. Optimisation of ultrasound-assisted extraction of natural pigment from annatto seeds by response surface methodology (RSM). Food Chem. 155, 319–324. https://doi.org/10.1016/j.foodchem.2014.01.059.

Zagklis, D.P., Paraskeva, C.A., 2018. Isolation of organic compounds with high added values from agro-industrial solid wastes. J. Environ. Manag. 216, 183–191. https://doi.org/10.1016/j.jenvman.2017.04.083.

Zagklis, D.P., Vavouraki, A.I., Kornaros, M.E., Paraskeva, C.A., 2015. Purification of olive mill wastewater phenols through membrane filtration and resin adsorption/desorption. J. Hazard Mater. 285, 69–76. https://doi.org/10.1016/j.jhazmat.2014.11.038.

Zhang, X., Cao, J., Jiang, L., Geng, C., Zhong, L., 2009. Protective effect of hydroxytyrosol against acrylamide-induced cytotoxicity and DNA damage in HepG2 cells. Mutat. Res. Fund Mol. Mech. Mutagen 664, 64–68. https://doi.org/10.1016/j.mrfmmm.2009.02.013.

Zhang, Y., Smuts, J.P., Dodbiba, E., Rangarajan, R., Lang, J.C., Armstrong, D.W., 2012. Degradation study of carnosic acid, carnosol, rosmarinic acid, and rosemary extract (*Rosmarinus officinalis* L.) assessed using HPLC. J. Agric. Food Chem. 60, 9305–9314. https://doi.org/10.1021/jf302179c.

Ziati, M., Khemmari, F., Cherifi, O., Didouche, F.-Y., 2017. Removal of polyphenols from olive mill wastewater by adsorption on activated carbon prepared from peach stones. Rev. Roum. Chem. 62, 865–874.